

## ARTICLE

## OPEN



# Critical role of translocator protein (TSPO) in neuronal mitochondrial dysfunction and mental stress-exacerbated ischemic injury following stroke

Yuequan Zhu<sup>1,5</sup>, Fengwu Li<sup>1,5</sup>, Omar Elmadhoun<sup>2</sup>, Qi Pang<sup>3</sup>, Yuchuan Ding<sup>1,3,4</sup> and Xiaokun Geng<sup>1,3,4</sup>

© The Author(s) 2025

Stroke remains the second leading cause of death and disability globally, yet the contribution of depressive disorders and psychological stress to stroke outcomes is often overlooked. Emerging evidence suggests that mitochondrial dysfunction may mediate this relationship. So this study aims to investigate the potential causal role of mental stress in exacerbating ischemic brain injury and identify mitochondrial proteins that contribute to this interaction. In the study, the chronic restraint stress (CRS) model was applied, and mice were subjected to 45 min of middle cerebral artery occlusion (MCAO) followed by 24 h or 48 h of reperfusion. Translocator protein (TSPO) antagonist PK11195 was injected intraperitoneally every day during CRS. Brain injury was determined by infarct volumes, cell apoptosis, Fas expression, release of lactate dehydrogenase (LDH), and reactive oxygen species (ROS). Protein expression was analyzed by Western blot. In SH-SY5Y cells, cell viability was assessed after oxygen-glucose deprivation/reoxygenation (OGD/R). Mitochondrial function was assessed after transfecting a TSPO overexpression vector (pLV-TSPO) or treated with PK11195. The results shown that CRS induced depressive-like behaviors and increased brain injury after stroke in association with impaired mitochondrial function. TSPO was elevated by CRS, and TSPO induced voltage-dependent anion channel (VDAC) phosphorylation through interaction with acyl-CoA binding domain containing 3 (ACBD3), which was reversed by PK11195. In SH-SY5Y cells, TSPO overexpression led to mitochondrial dysfunction, which was reversed by PK11195. In conclusion, the study supports a central role for TSPO in linking mental stress to adverse stroke outcomes and points to its potential as a therapeutic target for cerebrovascular health.

*Translational Psychiatry* (2026)16:9; <https://doi.org/10.1038/s41398-025-03745-1>

## INTRODUCTION

Stroke remains a major global health challenge, ranking as the second leading cause of death and a significant driver of long-term disability [1–3]. While vascular risk factors are well-established, growing attention is being directed toward modifiable nontraditional contributors such as depression [4, 5]. Given that depression affects over 264 million people globally, it has increasingly been recognized as a significant risk factor for ischemic stroke. In fact, a meta-analysis reported that individuals with depression have a 41% higher risk of experiencing a stroke compared to those without depression, highlighting the importance of depression as a variable risk factor in stroke prevention strategies [6]. Moreover, a cohort study published in *JAMA* observed a 67% increase in stroke incidence among individuals younger than 55 years between 2002–2010 and 2010–2018 [7]. Interestingly, the incidence of disability or fatal strokes, as determined by the National Institutes of Health Stroke Scale (NIHSS), was higher in the younger group (<55 years of age) compared with the older group (≥55 years). While risk factors such as low physical activity levels remained relatively stable for

patients under 55 years old, an exception was depression. These findings support the notion that mental stress plays a significant role in the onset and progression of stroke, particularly in younger individuals.

Mental stress activates the hypothalamic–pituitary–adrenal (HPA) axis and the sympathetic adrenal–medullary (SAM) axis, triggering a cascade of stress responses that increase the workload on mitochondria and disrupt cellular metabolic balance [8, 9]. As a result, chronic stress depletes mitochondrial adenosine triphosphate (ATP) reserves, leading to functional decline [10, 11]. Moreover, mitochondria play a key role in ischemia/reperfusion injuries, where their functional state significantly influences stroke severity [12, 13]. Together with their role in stress responses, this positions mitochondrial function as a potential link between mental stress and adverse stroke outcomes.

The translocator protein (TSPO), previously named the peripheral benzodiazepine receptor, is an 18-kDa protein located on the outer mitochondrial membrane, and is highly conserved across species [14, 15]. TSPO is critically involved in cholesterol transport, mitochondrial bioenergetics, and neurosteroid biosynthesis.

<sup>1</sup>Luhe Institute of Neuroscience, Capital Medical University, Beijing, China. <sup>2</sup>Division of Critical Care, Department of Anesthesiology & Perioperative Medicine Mayo Clinic, Rochester, MN, USA. <sup>3</sup>Department of Neurosurgery, Wayne State University School of Medicine, Detroit, MI, USA. <sup>4</sup>Department of Neurology and Stroke Intervention and Translational Center (SITC), Beijing Luhe Hospital, Capital Medical University, Beijing, China. <sup>5</sup>These authors contributed equally: Yuequan Zhu, Fengwu Li.

✉email: yding@med.wayne.edu; xgeng@ccmu.edu.cn

Received: 28 April 2025 Revised: 24 October 2025 Accepted: 7 November 2025  
Published online: 01 December 2025

Recent studies have further established that TSPO modulates mitochondrial function, redox homeostasis, microglial activation, synaptic pruning, and neuronal plasticity, all of which are key determinants of cellular energetics and resilience to stress [16–18]. Increased TSPO expression has been documented in the context of neuroinflammation and brain injury, including experimental models of ischemic stroke [19]. Moreover, positron emission tomography (PET) imaging studies have demonstrated elevated TSPO binding in the brains of patients with major depressive disorder (MDD) [20], as well as other psychological disorders, such as obsessive-compulsive disorder (OCD) and posttraumatic stress disorder (PTSD) [21]. Taken together, these findings support the central role of TSPO in linking mitochondrial dysfunction, neuroinflammation, and neuropsychiatric disorders.

Although mitochondrial dysfunction itself is well-established in ischemic stroke, we specifically chose TSPO as a target because recent evidence indicates that TSPO elevation precedes mitochondrial impairment, amplifies reactive oxygen species (ROS) generation, and increases susceptibility to calcium-induced mitochondrial permeability transition, thereby exacerbating neuronal injury [22]. Moreover, imaging studies using [<sup>18</sup>F]-FEDAC-PET have demonstrated rapid and localized TSPO overexpression colocalized specifically with activated microglia and dysfunctional mitochondria [23, 24]. Given these unique temporal and mechanistic insights, TSPO represents a particularly attractive therapeutic target to mitigate the exacerbation of stroke outcomes under conditions of mental stress. Mechanistically, TSPO interacts with A-kinase anchoring protein acyl-CoA binding domain containing 3 (ACBD3) [25], which activates protein kinase A (PKA) and leads to phosphorylation of the voltage-dependent anion channel (VDAC) [26]. Consequently, this phosphorylation event may increase mitochondrial permeability and sensitize cells to oxidant stress injury [27]. By elucidating these mechanisms, our study provides insight into potential pharmacological strategies that improve neuronal resilience and support functional recovery in stroke.

This study began with in vivo experiments, as the primary objectives was to determine the causal relationship between chronic stress and exacerbated ischemic injuries in animals and to identify key molecular contributors under physiologically relevant conditions. Once this phenomenon was demonstrated in vivo, we employed bioinformatic analyses to systematically screen for candidate molecules and pathways potentially mediating the observed effects. Finally, to validate the specificity and mechanistic role of TSPO-dependent pathway in neurons, we conducted in vitro cell culture experiments. The hypothesis tested was that mental stress-induced TSPO expression exacerbates stroke injury by promoting mitochondrial dysfunction through the ACBD3/PKA-VDAC phosphorylation pathway. Understanding this signaling cascade may help identify therapeutic targets to counteract the harmful effects of mental stress on cerebrovascular health.

## MATERIALS AND METHODS

### Animals

The animal protocol was approved by the Capital Medical University Laboratory Animal Welfare and Ethical Review Board under protocol number AEEL-2022-265 and was conducted in accordance with the NIH Guide for the Care and Use of Laboratory Animals for three times independently. A total of 169 adult, 6-week-old male C57BL/6J mice (20–22 g, Vital River Laboratory Animal Technology Co. Ltd, Beijing, China) were used in this study. In Experimental I, we determined the effect of stress on mitochondrial dysfunction and TSPO regulated pathway in the following four groups: (1) control (n = 14, 8 for Western blot and ELISA, and 6 for immunofluorescence); (2) CRS (n = 14, 8 for Western blot and ELISA, and 6 for immunofluorescence); (3) normal mice with PK11195 (inhibitor of TSPO) (n = 8 for Western blot and ELISA); (4) CRS mice+PK11195 (n = 8 for Western blot and ELISA). To verify the effects of CRS on ischemia stroke injuries and the intervention of TSPO inhibitors, we established a transient middle-cerebral-artery occlusion (MCAO) model on the above four groups

and added a sham operation group in Experimental II, including: (a) sham (no CRS and no MCAO) (n = 22, 8 for Western blot and ELISA, 8 for TTC, 6 for immunofluorescence and TUNEL); (b) MCAO without pre-CRS (n = 22, 8 for Western blot and ELISA, 8 for TTC, 6 for immunofluorescence and TUNEL); (c) MCAO with pre-CRS (n = 22, 8 for Western blot and ELISA, 8 for TTC, 6 for immunofluorescence and TUNEL); (d) MCAO + PK11195 without pre-CRS (n = 22, 8 for Western blot and ELISA, 8 for TTC, 6 for immunofluorescence and TUNEL); (e) MCAO + PK11195 with pre-CRS (n = 22, 8 for Western blot and ELISA, 8 for TTC, 6 for immunofluorescence and TUNEL). Animals (~ 10%) were excluded from further analysis due to death, brain hemorrhage, or lack of ischemic injuries based on neurological deficits and confirmed infarct volume. The investigator was blinded during the experiment and data assessment, and the timeline is shown in Fig. 1A.

### Chronic restraint stress (CRS)

CRS was conducted as previously described [28, 29]. Briefly, mice were randomly divided into CRS and control groups. Mice in the CRS group were placed in a well-ventilated Plexiglas tube (inner diameter, 6 cm) without food and water for 6 h per day (09:00 to 15:00), daily for 28 consecutive days. During the same time, control animals were kept in their home cages without food or water. Behavioral tests were then performed starting from Day 29.

### Administration of PK11195

The TSPO antagonist PK11195 (HY-19567, MCE) was administered intraperitoneally (IP) daily for 28 consecutive days, beginning prior to the onset of restraint stress. The dose of PK11195 (3 mg/kg) was chosen based on a previous study [30]. PK11195 was diluted to a concentration of 1.7 mM, and based on a body weight of 20–22 g, each mouse received a total volume of 100  $\mu$ l.

### Behavior Tests

**Open Field Test (OFT).** OFT was conducted as described previously [28]. Twenty-four hours after the last stress session, mouse behavior was monitored for 10 min using a digital camera. Images were captured with the SMART 3.0 animal behavior recording and analysis system (Panlab, Spain). The distances traveled and time spent in the central area (12.5  $\times$  12.5 cm) were calculated.

**Sucrose Preference Test (SPT).** SPT was conducted as previously reported [28]. Briefly, 24 h after the last stress session, mice were acclimated to a 1% sucrose solution (w/v) for 24 h, with two bottles of 1% sucrose solution in each cage. On the second day, a bottle of 1% sucrose solution and a bottle of water were provided. Following food and water deprivation, mice were given both sucrose solution and water for 24 h. Consumption was measured as: Sucrose Preference Ratio (%) = sucrose intake (g)/[sucrose intake(g) + water (g)]  $\times$  100%.

**Tail Suspension Test (TST).** TST was conducted as previously described [31]. The distal one-third of the mouse tail was taped and suspended from a support, with the head positioned 15 cm above the surface. After 6 min, immobility time was measured during the following 4 min (minutes 3–6) using the SMART 3.0 animal behavior system.

**Forced Swimming Test (FST).** FST was performed as described previously [31]. Mice were placed in an 18  $\times$  50 cm (diameter  $\times$  height) container of water for 6 min. Immobility time was measured for 4 min (minutes 3–6) using the SMART 3.0 system.

### Focal cerebral ischemia

Focal cerebral ischemia was induced as previously described [32, 33]. MCAO was performed with a 6–0 filament (Doccol Corporation, Sharon, MA, USA). A silicone-coated monofilament was gently introduced 10 mm distal to the external carotid/internal carotid bifurcation. During pre- and post-stroke surgery, we monitored cerebral blood flow using laser Doppler flowmetry (Perimed Periflux System 5000), confirming a stable drop in regional cerebral blood flow to approximately 12% of pre-occlusion baseline [33]. After 45 min of MCAO, mice were re-anesthetized, and the filament was gently withdrawn back into the common carotid artery to allow reperfusion. Exposure of the right MCA without occlusion served as sham surgery. The perioperative mortality associated with MCAO surgery (due to intracranial hemorrhage or anesthesia intolerance) was approximately 5%.

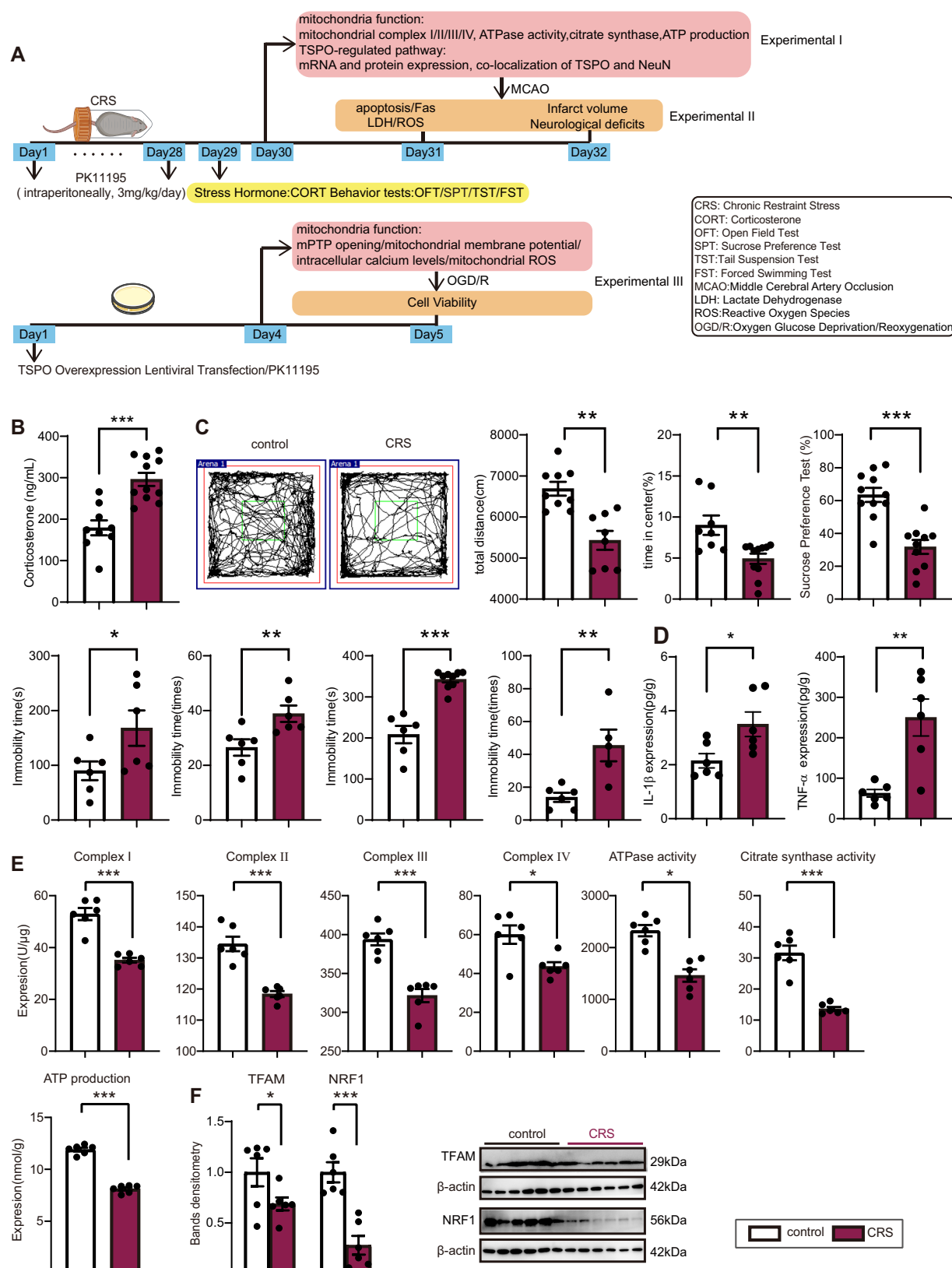


**Fig. 1 Mitochondrial Dysfunction upon Chronic Restraint Stress (CRS).** **A** Timeline of the study. **B** CRS increased corticosterone level in the serum ( $p < 0.001$ ). **C** CRS induced a decrease in the total distance and time in the center in the open field test (OFT) ( $p < 0.01$ ), the sucrose intake ratio in the sucrose preference test ( $p < 0.001$ ), increased immobility time in the tail suspension test (TST) ( $p < 0.01$ ) and forced swimming test (FST) ( $p < 0.001$ ). **D** The expressions of IL-1 $\beta$  ( $p < 0.05$ ) and TNF- $\alpha$  ( $p < 0.01$ ) in brain were significantly increased upon CRS. **E** CRS decreased the activities of mitochondria respiratory complex I/II/III/IV ( $p < 0.001$ ), ATPase ( $p < 0.05$ ), citrate synthase ( $p < 0.001$ ), and the amount of ATP production ( $p < 0.001$ ). **F** CRS induced reduction of TFAM ( $p < 0.05$ ) and NRF1 ( $p < 0.001$ ). Data are presented as mean  $\pm$  SEM.

**Table 1.** Primer sequences of Real-time PCR.

Name	Forward Primer	Reverse Primer
TSPO mouse	GCCTACTTTGTACGTGGCGAG	CCTCCAGCTTCCAGAC
TSPO human	CCTGCTCTACCCCTACCTGG	GCCATACGCAGTAGTTGAGTG
β-actin	GTGACGTTGACATCCGAAAGA	GCGGACTCATCGTACTCC

### Neurological deficits and infarct volume

Neurological deficits were evaluated 24 h after reperfusion using 5-point and 12-point neurological scoring systems as previously described [34, 35]. Mice scoring  $\leq 2$  due to failed surgery were excluded (~5%). For 2, 3, 5-triphenyl tetrazolium chloride (TTC) staining, mice were sacrificed 48 h after MCAO, and the brains were sliced into six 1 mm-thick coronal sections. For each slice, the infarct volume was calculated by Image J software, ensuring that reported infarct sizes reflect true tissue loss rather than edema-related enlargement. The calculation formula is as follows:

$$\text{Infarct volume (\%)} = [(\text{total left hemisphere volume}) - (\text{non-infarcted right hemisphere volume})] / \text{total left hemisphere volume} \times 100\%.$$

### Enzyme-linked immunosorbent assay (ELISA)

ELISA was performed as previously described [36]. ELISA kits were used to measure Fas expression (ml063244, MLBIO), ROS (ml009876-1, MLBIO), lactate dehydrogenase (LDH) release (ml002267, MLBIO), corticosterone (CORT) (ml037564, MLBIO), interleukin-1 beta (IL-1 $\beta$ , ml098416, MLBIO), tumor necrosis factor- $\alpha$  (TNF- $\alpha$ , ml002095, MLBIO), mitochondria complex I activity (ml723552, MLBIO), mitochondria complex II activity (ml723412, MLBIO), mitochondria complex III activity (ml728752, MLBIO), mitochondria complex IV activity (ml723413, MLBIO), ATPase activity (ml720029, MLBIO), citrate synthase activity (ml722662, MLBIO) and ATP production (YY571120, MLBIO). Absorbance at 405 nm was recorded using a microplate reader (Thermo, USA).

### Terminal uridine nick-end labeling (TUNEL) assay

TUNEL staining was performed using the In Situ Cell Death Detection Kit, Fluorescein (Roche), as previously described [37]. TUNEL-positive cells were counted using the manual cell counting tool in Image J.

### Bioinformatics analysis

Candidate genes related to ischemic stroke and mental stress were identified using DisGeNet (<https://www.disgenet.org/>). Mitochondrial genes in mice were retrieved from the MitoCarta3.0 database (<https://www.broadinstitute.org/mitocarta>). Bioinformatic analyses were performed using OECloud tools (<https://cloud.oebiotech.com>).

### Western blotting

Western blotting was conducted as previously described [38]. Primary antibodies included: anti-TSPO (1:1000, ab109497, Abcam), anti-ACBD3 (1:500, 14096-1-AP, Proteintech), anti-PKA (1:1000, PTM-7162, PTM Bio Inc), anti-Calcium/Cammodulin-dependent Kinase (CaMK) (1:1000, PTM-6045, PTM Bio Inc), anti-mitochondrial transcription factor A (TFAM) (1:1000, ab307302, Abcam), anti-nuclear respiratory factor 1 (NRF1) (1:1000, ab158926, Absin), and anti-β-actin (1:5000, A5060, Sigma-Aldrich). Protein quantification was performed using Image J.

### Real-time PCR

Total RNA was isolated with TRIzol reagent (Invitrogen, Carlsbad, CA, USA) according to the manufacturer's protocol. One  $\mu$ g of RNA was reverse-transcribed into cDNA. Quantitative PCR was then performed on an ABI PRISM 7500 real-time system (Applied Biosystems). Transcript levels of TSPO and β-actin were determined with the  $2^{-\Delta\Delta CT}$  method [39, 40]. Primer sequences are listed in Table 1.

### Immunofluorescence

Immunofluorescence assays were used to assess TSPO-NeuN and PKA-DAPI co-localization [41]. After behavioral testing, brain tissues were collected, dehydrated, paraffin-embedded, and cut into 5  $\mu$ m sections. Sections were incubated overnight at 4 °C with the following primary antibodies: anti-TSPO antibodies (1:200, ab109497, Abcam), anti-PKA (1:1000, PTM-7162), anti-NeuN antibodies (1:200, ab104224, Abcam). TSPO+NeuN+cells were counted using Image J.

### Co-immunoprecipitation (Co-IP)

Co-IP of ACBD3 and TSPO, VDAC phosphorylation and TSPO was performed as previously described [37]. Brain tissue lysates were collected using immunoprecipitation (IP) lysis buffer and centrifuged. Primary antibodies were added and incubated at 4 °C overnight: anti-VDAC (1:500, 66345-1-Ig, Proteintech), anti-ACBD3 (1:500, 14096-1-AP, Proteintech), anti-TSPO (66345-1-Ig, Proteintech), anti-pan phospho-serine/threonine (1:500, AP0893, abclonal), and IgG antibody (1:1000, 2729, Cell Signaling Technology). Protein G magnetic beads were added, and magnetic separation was performed using a Magnetic Separation Rack (7017, CST). Immunocomplexes were boiled and analyzed by Western blot.

### SH-SY5Y Cell culture

The human SH-SY5Y neuroblastoma cell line (CRL-2266, ATCC) was cultured in 25 cm<sup>2</sup> tissue culture flasks (T25) containing 12–15 mL of DMEM/F12 medium (Thermo Fisher Scientific) supplemented with 10% fetal bovine serum (FBS, Thermo Fisher Scientific). Cells were maintained at 37 °C in a humidified incubator with 5% CO<sub>2</sub> and used between passages 9 and 11, as previously described by our group [36].

### Oxygen glucose deprivation/reoxygenation (OGD/R)

Oxygen glucose deprivation (OGD) was performed using a hypoxic chamber flushed with 5% CO<sub>2</sub> and 95% N<sub>2</sub> and maintained at 37 °C [36]. Culture medium was replaced with deoxygenated, glucose-free DMEM (Gibco) to initiate OGD for 2 h. Following OGD, cells were returned to normoxic conditions, and the medium was replaced with standard maintenance medium. Cells were incubated for either 6 h or 24 h prior to harvest for downstream analyses as shown as Experiment III in Fig. 1A.

### Lentiviral transfection of TSPO in SH-SY5Y cells

Lentiviral construct with TSPO, pLV-hef1a-mNeongreen-P2A-Puro-WPRE-CMV-TSPO (Human, NM\_001256530) (Beijing Syngentech Co., LTD), was used for TSPO overexpression in SH-SY5Y cells (vector ID of pHS-AVC-1244). The TSPO coding sequence [NM\_001256530] was injected into the construct with CMV promoter. Lentivirus containing TSPO or the corresponding control vector (vector ID of pHs-B-0080) was transfected into cells at a multiplicity of infection (MOI) of 4. Cells were incubated at 37 °C for 24, 48 and 72 h, with fresh medium changed at each time point [42].

### Mitochondria function

*Assessment of mPTP opening.* The opening of mitochondrial permeability transition pores (mPTP) was detected using mPTP Assay Kit (Beyotime), as previously reported [43]. Briefly, treated cells were washed with PBS and incubated with calcine AM plus Co<sup>2+</sup> quencher at 37 °C for 30 min. The dye was then replaced by culture medium, and the slides were cultured at 37 °C for 30 min in the dark and observed by flow cytometer and microplate reader at 494/517 nm (Ex/Em) absorbance.

*Mitochondrial membrane potential (MMP) by JC-1 staining.* MMP was measured using a JC-1 Assay Kit (Invitrogen, T-3168), as previously reported [44]. Cells were incubated with JC1 dye (5  $\mu$ M) for 30 min at 37 °C. The dye accumulates in mitochondria in a potential-dependent manner, resulting in a fluorescence shift from green (Ex 485 nm/Em 516 nm) to red (Ex 579 nm/Em 599 nm). MMP was quantified using a microplate reader.

*Intracellular calcium ion levels by Fluo-4 staining.* Intracellular calcium levels were measured using the Fluo-4 Calcium Assay Kit (Beyotime) as previously described [45]. Cells were washed three times with PBS and incubated with Fluo-4 AM solution (500  $\mu$ L per well) for 30 min at 37 °C. After incubation, cells were washed three additional times. Fluorescence intensity was recorded using a flow cytometer (C6, BD, USA), and the fluorescence ratio was analyzed at 488 nm excitation using a microplate reader.

**Mitochondrial ROS assessment by mito-SOX staining.** Mitochondrial ROS levels were detected using the mito-SOX reagent (M36008, Thermo Fisher, USA) as previously reported [45]. A 5  $\mu$ M working solution of mito-SOX was prepared, and 1.0 mL of the 5  $\mu$ M mito-SOX reagent was applied as a cell-loading solution. Cells were incubated for 10 min at 37 °C in the dark. Fluorescence was measured at 510/580 nm (Ex/Em) absorbance using a microplate reader.

#### Water-soluble tetrazolium salt-1 (WST-1) Assay

WST-1 assay (Roche Diagnostic, Germany) was performed according to the manufacturer's instructions to evaluate cell viability, as previously described [46]. Transparent 96-well plates with culture media (100  $\mu$ L) were prepared and 10  $\mu$ L of WST-1 reagent was added. Plates were incubated for 1 h in a standard incubator and shaken for 1 min prior to absorbance measurement at 450 nm using a microplate reader. Each test was performed in triplicate and independently repeated 6 times.

#### Statistical analysis

Sample size analysis was performed using G\*Power software 3.1 (University of Kiel, Germany). The data in each group were confirmed to follow a normal distribution. After two-way ANOVA revealed a significant interaction, post-hoc comparisons were performed with Tukey's multiple-comparisons test to isolate group differences. All post-hoc tests were two-tailed and corrected for multiplicity;  $p < 0.05$  was considered significant. All data are expressed as mean  $\pm$  standard error (SE). Statistical analyses were run in GraphPad Prism 8.0 (San Diego, CA, USA).

## RESULTS

#### Depressive-like behaviors after CRS

The effectiveness of CRS was confirmed by a comprehensive series of stress-related hormones and behavioral tests, including the open field test (OFT), sucrose preference test (SPT), tail suspension test (TST), and forced swim test (FST). The corticosterone (CORT) level in serum was increased to 296.1 ng/mL in the CRS group, compared to 179.1 ng/mL in the control group (Fig. 1B,  $p < 0.001$ ), suggesting that CRS could activate the hypothalamic-pituitary-adrenal (HPA) axis significantly. Representative running paths from the OFT are shown in Fig. 1C. Notably, CRS-exposed animals exhibited a significant reduction in total distance traveled and time spent in the center of the arena during the OFT ( $p < 0.01$ ). In addition, the sucrose preference ratio in the SPT was significantly decreased ( $p < 0.001$ ), indicating a loss of interest in pleasurable activities. Similarly, immobility time was markedly prolonged in both TST ( $p < 0.01$ ) and FST ( $p < 0.001$ ). IL-1 $\beta$  and TNF- $\alpha$  are key neuroinflammatory markers and pro-inflammatory cytokines [47]. To clarify whether CRS could induce neuroinflammation, we examined the expression levels of IL-1 $\beta$  and TNF- $\alpha$  in brain tissues through ELISA. The results showed that CRS significantly upregulated the expression of IL-1 $\beta$  ( $p < 0.05$ ) and TNF- $\alpha$  (Fig. 1D,  $p < 0.01$ ) in the brain, indicating that CRS induces a robust neuroinflammatory response.

#### Mitochondrial dysfunction after CRS

The activity of mitochondrial respiratory complexes I/II/III/IV, mitochondrial ATPase, citrate synthase (CS) activity, and ATP production were measured to determine mitochondrial function following CRS. At 24 h post-CRS, the activities of mitochondrial complex I/II/III/IV were significantly decreased in the entire brain ( $p < 0.001$ ). In addition, reductions were observed in ATPase activity ( $p < 0.05$ ), CS activity ( $p < 0.001$ ), and total ATP production (Fig. 1E,  $p < 0.001$ ). Collectively, these findings suggest that psychological stress impairs the activity of the mitochondrial respiratory chain and reduces ATP production in the brain.

#### Suppressed mitochondrial biogenesis after CRS

In addition to mitochondrial respiratory chain complex activity and ATP synthesis, mitochondrial biogenesis is essential for maintaining both the quantity and quality of mitochondria [48].

Mitochondrial transcription factor A (TFAM) and nuclear respiratory factor 1 (NRF1), two critical biomarkers of mitochondrial biogenesis [49, 50], were assessed in the CRS model. CRS significantly reduced TFAM ( $p < 0.05$ ) and NRF1 ( $p < 0.001$ ) expression. Collectively, these findings indicate that CRS suppresses not only respiratory-chain complex activity and ATP production but also mitochondrial biogenesis.

#### Aggravated stroke injuries by CRS

As we demonstrated in Experiment I, CRS impaired mitochondrial respiratory chain activity and suppressed mitochondrial biogenesis. Given the established role of mitochondrial dysfunction in influencing stroke outcomes [48], Experiment II was conducted to further assess whether CRS aggravated ischemic injury and whether TSPO inhibition ameliorated these effects. We established a MCAO model in both the control and CRS group and measured the infarct volume and neurological deficits at 24/48 h after reperfusion. A sham group was set as a negative control to rule out the effects of the surgical procedure. The results showed that CRS resulted in a marked increase in infarct volume following stroke with infarct volume increasing from 31.4% to 53.1% (Fig. 2A,  $p < 0.001$ ). Neurological deficits, evaluated using both 5-point and 12-point scoring systems, were significantly worsened by CRS ( $p < 0.01$ ). Moreover, a significant negative correlation between the sucrose preference test (SPT) ratio pre-stroke and MCAO induced infarct volume was observed ( $p = 0.0011$ ), suggesting that higher levels of stress are associated with larger infarct volumes following ischemic stroke (Fig. 2B,  $p < 0.01$ ). These findings indicate that pre-stroke CRS exacerbated ischemic injury.

#### Apoptosis and production of ROS and LDH in stroke by CRS

CRS also enhanced MCAO-induced Fas expression, a key marker of apoptosis (Fig. 2C,  $p < 0.001$ ), and led to elevated levels of ROS ( $p < 0.01$ ) and LDH ( $p < 0.001$ ) in the brain. Consistent with these findings, TUNEL staining revealed that apoptotic cell death in the MCAO-affected region was significantly increased in the CRS group, as evidenced by a higher proportion of TUNEL-positive cells (Fig. 2D,  $p < 0.001$ ). These findings demonstrate that pre-stroke CRS amplifies apoptosis, oxidative stress, and cellular damage following ischemic insult.

#### Translocator protein (TSPO) expression in the brain

The hub molecules linking psychological stress and cerebrovascular injury were identified through database prediction, followed by Western blot and immunofluorescence. Analysis of the DisGeNet database identified 330 genes associated with ischemic stroke and 501 with depression, with an overlap of 158 genes. Subsequently, cross-referencing these genes with the MitoCarta3.0 database for mice revealed three candidate genes: Translocator protein (TSPO), B cell leukemia/lymphoma 2 (BCL2), and DNA polymerase delta interacting protein 2 (POLDIP2). Among these, BCL2 and POLDIP2 were primarily associated with apoptotic cell death and DNA replication/repair, respectively. These findings suggest that TSPO is a key molecular link connecting psychological stress, ischemic stroke, and mitochondrial dysfunction (Fig. 3A).

Consistent with this, TSPO expression was significantly upregulated in the whole brain following CRS, both at the mRNA ( $p < 0.001$ ) and protein levels (Fig. 3B,  $p < 0.01$ ), compared with the control group. Furthermore, immunofluorescence assays demonstrated that the CRS-increased TSPO expression was co-localized with NeuN, a neuronal marker (Fig. 3C). Specifically, the percentage of TSPO and NeuN co-localization was 58% higher under psychological stress (37% in the control group,  $p < 0.001$ ). Correlation analysis between the SPT ratio and TSPO expression levels in the pre-stroke stress model was conducted. The results showed a significant negative correlation (Fig. 3D,  $p < 0.01$ ). This indicates that stress-induced anhedonia was linked to increased

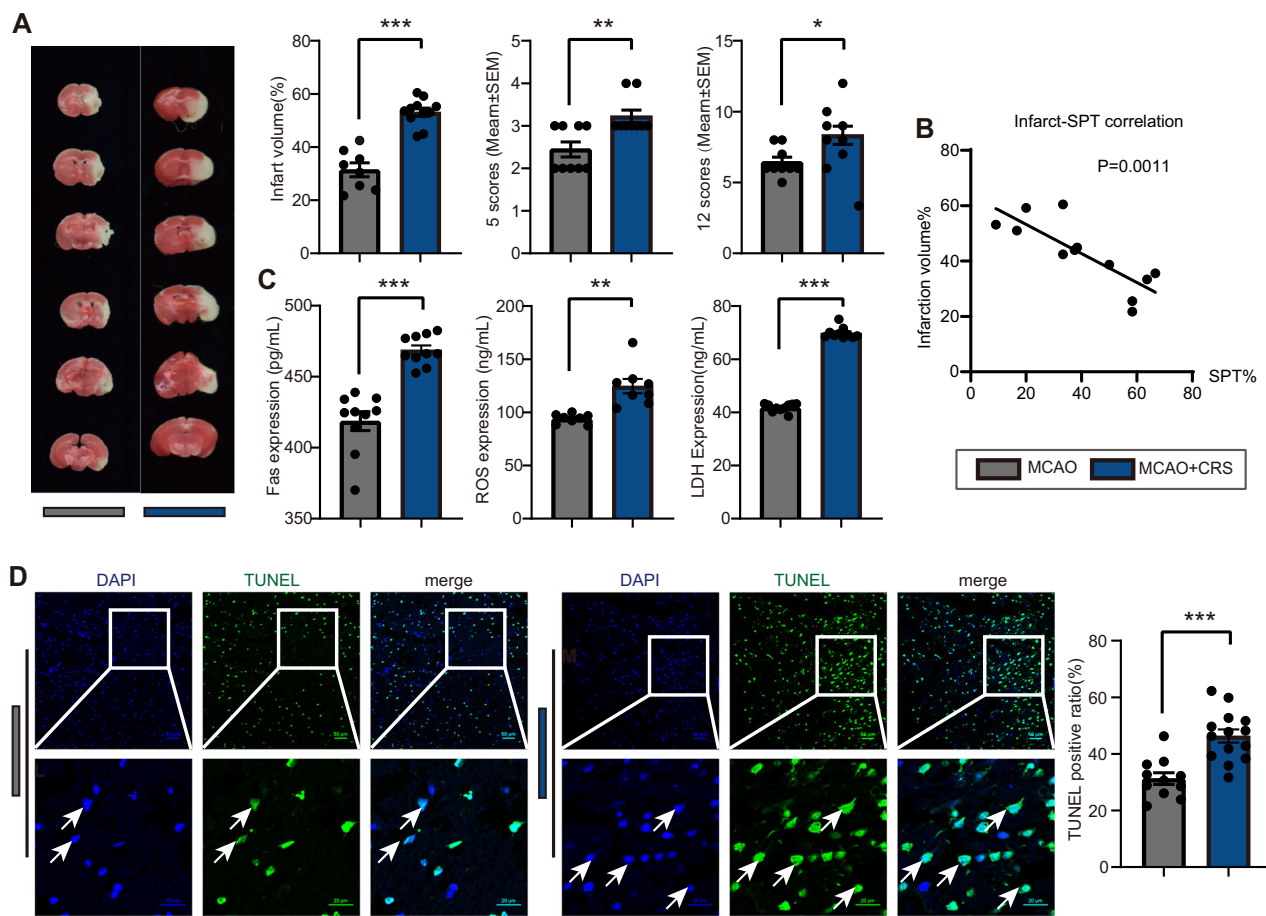


**Fig. 2 Stroke Injuries after middle cerebral artery occlusion (MCAO). A** The 2, 3, 5-Triphenyltetrazolium chloride (TTC) staining illustrated infarct volumes in MCAO with or without CRS at 48 h after reperfusion. CRS aggravated MCAO induced stroke injuries ( $p < 0.001$ ). Neurological deficits in MCAO were increased at 48 h after reperfusion by using 5 scores ( $p < 0.01$ ) and 12 scores system ( $p < 0.05$ ). **B** Lower sucrose preference is associated with larger infarct volumes following ischemic stroke. **C** The expressions of Fas, reactive oxygen species (ROS) and lactate dehydrogenase (LDH) were examined by ELISA, and CRS increased the expression of Fas ( $p < 0.001$ ), ROS ( $p < 0.01$ ) and LDH ( $p < 0.001$ ) in the brain. **D** CRS aggravated MCAO induced cell apoptosis and increased TUNEL positive ratio ( $p < 0.001$ ). Data are presented as mean  $\pm$  SEM.

TSPO expression. Collectively, this suggests that TSPO may serve as a molecular mediator through which psychological stress exacerbates stroke severity by promoting mitochondrial dysfunction in neurons.

#### ACBD3/PKA-VDAC phosphorylation CaMK signaling pathway after CRS

TSPO has been reported to interact with A-kinase anchoring protein acyl-CoA binding domain containing 3 (ACBD3), leading to the activation of protein kinase A (PKA) and subsequent phosphorylation of the voltage-dependent anion channel (VDAC). To further examine this interaction, binding between TSPO and ACBD3 was predicted using HDock (<http://hdock.phys.hust.edu.cn/>) and visualized with PyMOL (version 2.X, Schrödinger, LLC), both widely used tools for assessing ligand-macromolecule binding modes and affinities. From the prediction results, the model with the highest docking and confidence scores was selected, and its non-covalent interactions were visualized (Fig. 3E).

Consistent with these predictions, co-immunoprecipitation showed that TSPO-ACBD3 interaction was significantly enhanced under CRS conditions (Fig. 3F,  $p < 0.001$ ). Furthermore, the expression of ACBD3 was also upregulated in response to CRS (Fig. 3G,  $p < 0.001$ ).

Since ACBD3 is known to induce VDAC phosphorylation via PKA, we examined the downstream effects of this pathway.

Phosphorylated VDAC facilitates calcium transport across the mitochondrial outer membrane, thereby activating CaMK ( $p < 0.05$ ) and suggesting elevated calcium levels. Following CRS, both PKA protein expression and fluorescence-labeled neurons were increased (Fig. 3H,  $p < 0.01$ ), accompanied by VDAC phosphorylation detected by immunofluorescence and co-immunoprecipitation ( $p < 0.001$ ). Collectively, these findings indicate that TSPO activates the ACBD3/PKA-VDAC phosphorylation pathway and upregulates CaMK under psychological stress, resulting in TSPO-mediated mitochondrial dysfunction and exacerbated stroke injury after CRS.

#### Mitochondrial dysfunction using TSPO antagonist (PK11195) upon CRS

To delineate the key role of TSPO in brain injury under CRS, pharmacological inhibition of TSPO was implemented via systemic PK11195 administration during CRS in Experiment I. PK11195 has been systematically validated in rodents [51], non-human primates [52], and humans [53]. As expected, PK11195 significantly reduced the CRS-induced upregulation of TSPO expression (Fig. 4A,  $p < 0.05$ ). To further elucidate the mechanisms underlying the protective effects of TSPO inhibition, we assessed the activities of mitochondrial complexes I-IV in ischemic mice. PK11195 did not significantly affect mitochondrial complex I, II, III, and IV activities in ischemic mice without CRS,

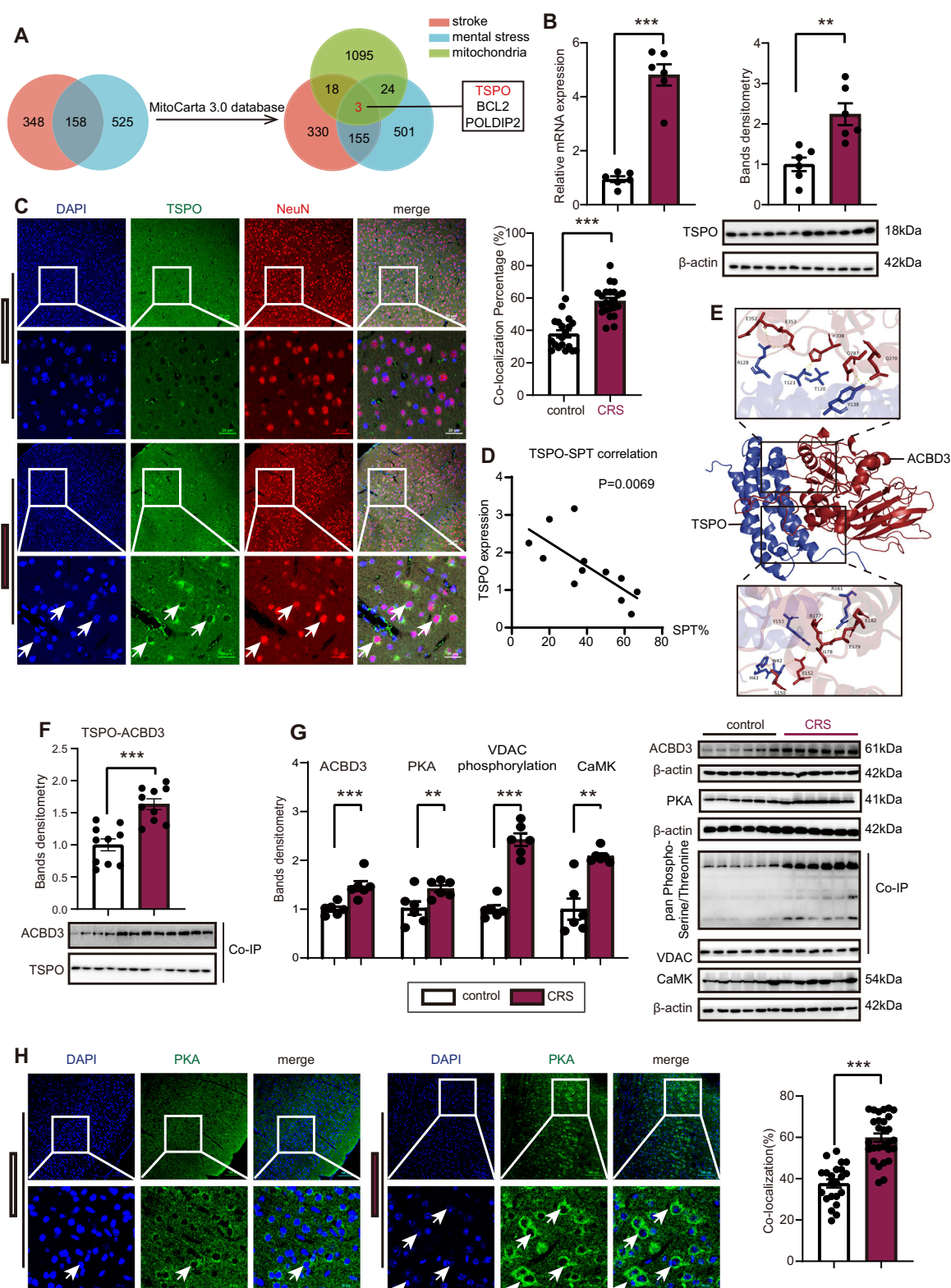


**Fig. 3 TSPO Expression in Brain and Activation of ACBD3/PKA-CaMK Pathway.** **A** Translocator protein (TSPO) was screened through the DisGeNet and MitoCarta3.0 database. **B** TSPO mRNA and protein expression were analyzed 24 h after CRS in the brain, and both mRNA and protein expression level of TSPO were increased upon CRS. **C** Green fluorescence, representing the expression of TSPO, and red fluorescence, representing the expression of NeuN (a neuronal marker) were co-localized, and the number of TSPO+NeuN+cells was increased upon CRS in the brain ( $p < 0.001$ ). **D** SPT ratio was negative correlated with TSPO expression. **E** Molecular docking prediction and visualization of binding interactions between TSPO and ACBD3. **F** The interaction between TSPO and ACBD3 was enhanced under CRS ( $p < 0.001$ ). **G** CRS increased the expression of ACBD3 ( $p < 0.001$ ), PKA ( $p < 0.01$ ), and CaMK ( $p < 0.01$ ), and phosphorylation of VDAC was increased upon CRS by Western blot and co-immunoprecipitation ( $p < 0.001$ ). **H** Fluorescence intensity of PKA was increased upon CRS ( $p < 0.001$ ). Data are presented as mean  $\pm$  SEM.

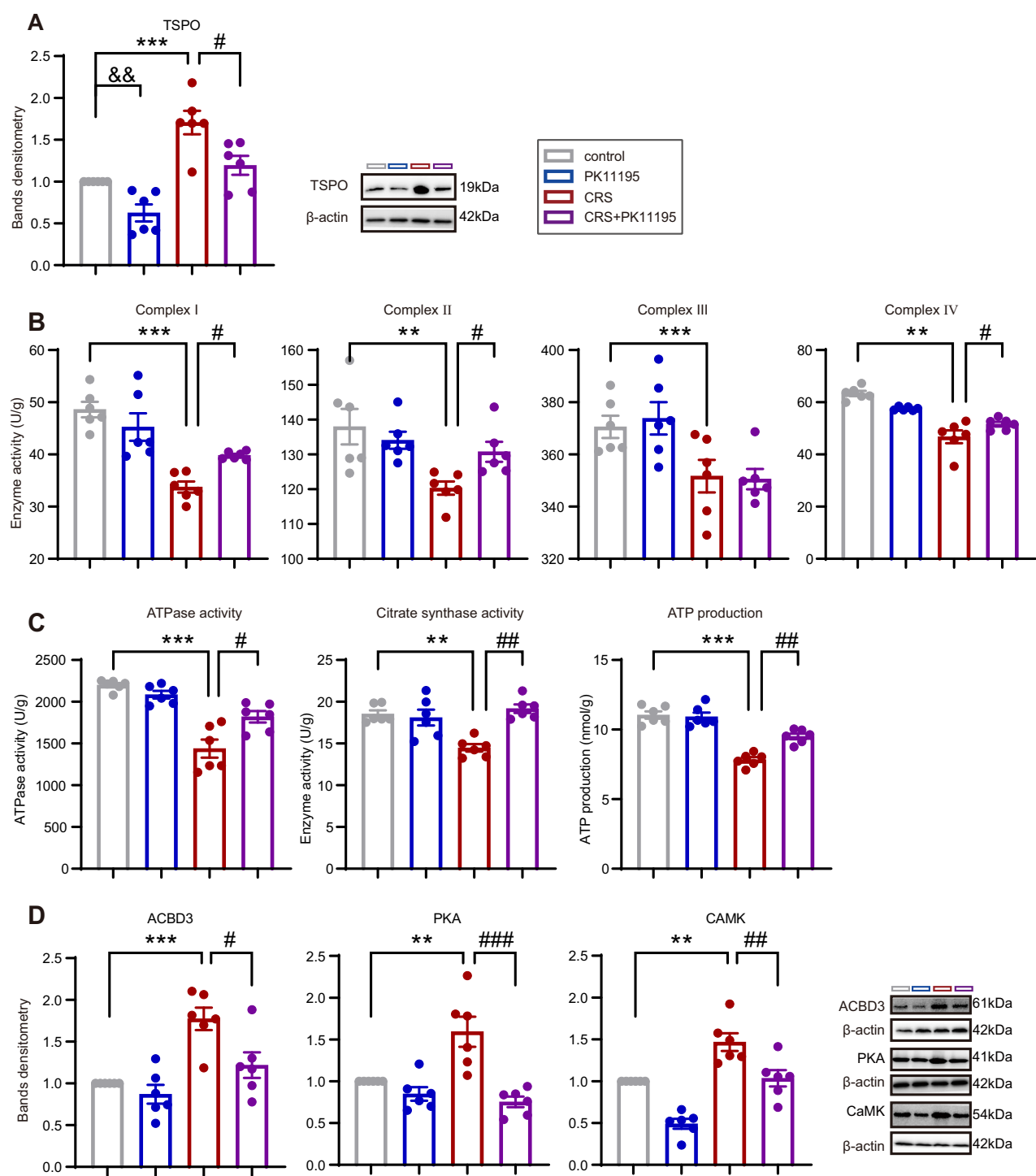


**Fig. 4 Rescued CRS aggravating Mitochondrial Dysfunction in the Brain by TSPO Antagonist (PK11195).** **A** Administration of PK11195 decreased mental-stress-induced upregulation of TSPO. **B** PK11195 alleviated CRS decreased the activities of mitochondria respiratory complex I/II/III/IV ( $p < 0.05$ ). **C** The activities of ATPase ( $p < 0.05$ ), citrate synthase ( $p < 0.01$ ), and ATP production ( $p < 0.01$ ) were rescued upon PK11195. **D** PK11195 reduced CRS-induced increases in the protein expression of ACBD3 ( $p < 0.05$ ), PKA ( $p < 0.001$ ) and CaMK ( $p < 0.01$ ) upon PK11195. \*: CRS vs control. &: control vs PK11195. #: CRS vs CRS + PK11195. Data are presented as mean  $\pm$  SEM.

while it reversed these reductions in MCAO mice following CRS (Fig. 4B,  $p < 0.05$ ). A similar restorative effect was observed on mitochondrial activities, including ATPase activity (Fig. 4C,  $p < 0.05$ ), CS activity ( $p < 0.01$ ), and total ATP production ( $p < 0.01$ ). These findings suggest that TSPO inhibition mitigates CRS-induced impairments in mitochondrial respiratory chain and ATP production in ischemic brain.

#### ACBD3/PKA-CaMK pathway by PK11195 upon CRS

We examined the effects of PK11195 on the ACBD3/PKA-CaMK signaling pathway, previously identified as central to TSPO-mediated stress-aggravated stroke injury. PK11195 markedly reduced CRS-induced upregulation of ACBD3 (Fig. 4D,  $p < 0.05$ ), PKA ( $p < 0.001$ ), and CaMK ( $p < 0.01$ ). These results support the role of the ACBD3/PKA-CaMK pathway in mediating the

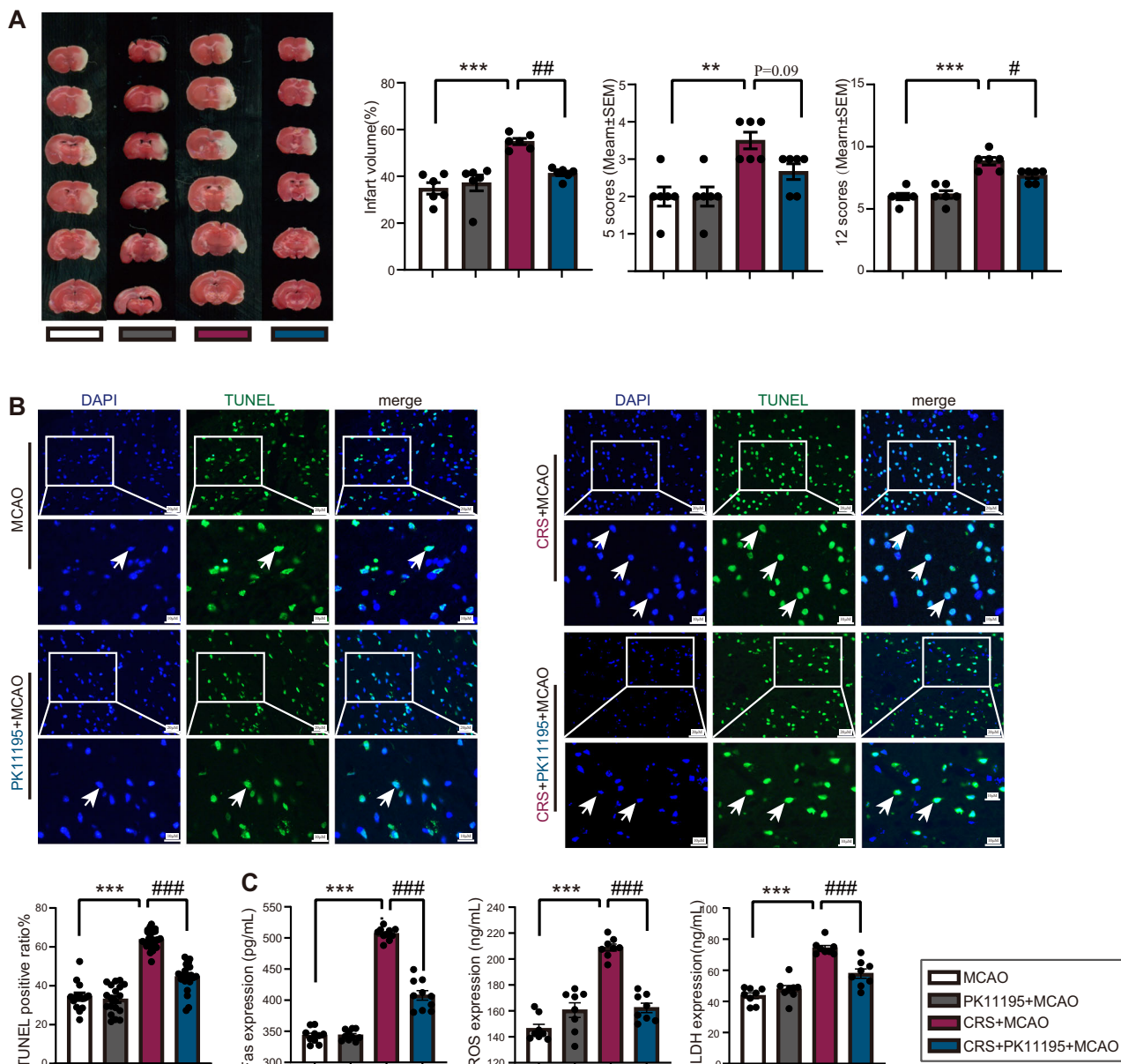


**Fig. 5 Reduced CRS aggravating Brain Damage in MCAO by PK11195.** **A** TTC staining illustrated infarct volumes in MCAO with or without TSPO antagonist (PK11195) at 48 h after reperfusion. PK11195 decreased mental stress-aggravated stroke injuries at 48 h after reperfusion ( $p < 0.01$ ). Neurological deficit in MCAO at 48 h after reperfusion by using the 5-point and 12-point scoring systems. PK11195 alleviated mental stress worsening neurological deficits in MCAO at 48 h after reperfusion ( $p < 0.05$ ). **B** TUNEL assay was tested at 24 h after reperfusion, showing PK11195 decreased the positive ratio of CRS aggravating apoptosis cells in brain after MCAO ( $p < 0.001$ ). **C** PK11195 decreased the increasing expression of Fas ( $p < 0.001$ ), ROS ( $p < 0.001$ ) and LDH ( $p < 0.001$ ) upon CRS in the brain. \*: CRS vs control. #: CRS vs CRS + PK11195. Data are presented as mean  $\pm$  SEM.

protective effects of TSPO inhibition against stress-aggravated stroke. Collectively, our findings underscore the critical role of TSPO in modulating psychological stress in the context of cerebrovascular disease.

#### Stroke damage and neurological deficits upon PK11195

The above findings confirmed that TSPO inhibition can rescue CRS-impaired mitochondrial function. To further assess whether PK11195 mitigates stress-exacerbated stroke damage, we administered it in both the MCAO group and the MCAO + CRS group and evaluated brain injury and neurological deficits in Experiment II. PK11195 treatment was associated with reduced infarct volume at 48 h post-reperfusion (Fig. 5A,  $p < 0.01$ ) and significantly improved neurological outcomes on both the 5-point and 12-

point scales ( $p < 0.05$ ). Notably, PK11195 did not confer neuroprotection in ischemic rats without prior CRS exposure. Collectively, these findings indicate that TSPO contributes specifically to stress-enhanced ischemic injury, underscoring its relevance in stress-aggravated cerebrovascular damage.

#### MCAO injuries after TSPO inhibition (PK11195)

Building on these findings, further investigation showed that PK11195 did not reduce cell death in ischemic mice without CRS, but significantly reduced CRS-aggravated apoptosis in the CRS + MCAO group (Fig. 5B,  $p < 0.001$ ), indicating that TSPO inhibition alleviated CRS-induced apoptotic cell death. Furthermore, PK11195 attenuated the CRS-aggravated upregulation of Fas expression at 24 h post-reperfusion (Fig. 5C,  $p < 0.001$ ). Similar

protective effects were observed for ROS ( $p < 0.001$ ) and LDH ( $p < 0.001$ ). These results suggest that TSPO inhibition selectively mitigates psychological stress-exacerbated ischemic injury.

#### Mitochondrial dysfunction in SH-SY5Y OGD/R model

To further validate the neuronal mechanisms underlying these findings, Experiment III was performed in SH-SY5Y cells to determine whether TSPO overexpression directly caused mitochondrial dysfunction, while PK11195 reversed these changes. Carbonyl cyanide m-chlorophenyl hydrazone (CCCP) is widely employed as a positive control for mitochondrial dysfunction because it rapidly dissipates mitochondrial membrane potential by uncoupling oxidative phosphorylation, thereby inducing mitochondrial damage [54]. Including CCCP in our experiments allowed us to validate the sensitivity and specificity of our mitochondrial function assays. As shown in Fig. 6, treatment with CCCP increased mitochondrial membrane potential, determined by JC1 staining (Fig. 6A,  $p < 0.001$ ). Cell viability, assessed by WST-1 assay, was significantly reduced at 6 and 24 h post-reoxygenation after 2 h of OGD and CCCP treatment ( $p < 0.001$ ). We next evaluated the protective effects of Mito-TEMPO, a mitochondria-targeted superoxide scavenger. Mito-TEMPO markedly improved mitochondrial membrane potential, as shown by the green/red fluorescence ratio in JC-1 staining (Fig. 6B,  $p < 0.01$ ), and significantly enhanced cell viability at both 6 and 24 h post-reoxygenation ( $p < 0.001$ ). These findings suggest that preserving mitochondrial function can attenuate OGD/R-induced neuronal injury.

#### Mitochondrial dysfunction after TSPO overexpression (pLV-TSPO) in SH-SY5Y cells

To further elucidate the role of TSPO in neurons, we constructed a TSPO overexpression vector (pLV-TSPO) and transfected it into SH-SY5Y cells (Fig. 6C) to observe the effects of TSPO on neuronal mitochondria. At 72 h post-transfection, TSPO expression was significantly upregulated at both mRNA (Fig. 6D,  $p < 0.001$ ) and protein levels ( $p < 0.01$ ), confirming successful overexpression of TSPO in the transfected cells. We then examined several key indicators of mitochondrial function and integrity. Overexpression of TSPO reduced mitochondrial permeability transition pore (mPTP) opening (Fig. 6E,  $p < 0.001$ ) while increasing intracellular calcium levels detected by the Fluo-4 probe ( $p < 0.01$ ), mitochondrial membrane potential (MMP) measured via JC-1 staining ( $p < 0.01$ ), and mitochondrial reactive oxygen species (mito-ROS), assessed using mito-SOX dye ( $p < 0.001$ ). These results indicate that TSPO overexpression causes mitochondrial dysfunction in SH-SY5Y cells. The observed changes in mPTP opening, intracellular calcium levels, MMP, and mto-ROS production highlight the complex and potentially detrimental effects of elevated TSPO levels on mitochondrial health.

#### Rescued mitochondrial function after PK11195 in SH-SY5Y cells

Given the marked mitochondrial dysfunction observed in SH-SY5Y cells overexpressing TSPO (pLV-TSPO), we investigated whether pharmacological inhibition of TSPO could counteract these effects. Accordingly, pLV-TSPO-transfected cells were treated with PK11195 to assess mitochondrial function. In these cells, PK11195 reversed reductions in mitochondrial permeability transition pore (mPTP) opening (Fig. 6F,  $p < 0.001$ ), intracellular  $\text{Ca}^{2+}$  levels ( $p < 0.01$ ), the green/red fluorescence ratio in JC-1 staining ( $p < 0.01$ ), and mitochondrial ROS levels ( $p < 0.01$ ). These results indicate that TSPO inhibition effectively alleviates TSPO-induced mitochondrial dysfunction. Taken together, these three experimental approaches provide converging evidence that stress-induced TSPO upregulation contributes to mitochondrial dysfunction and exacerbates stroke injury.

## DISCUSSION

In this study, we demonstrated a causal link between prior mental stress and ischemic stroke outcomes, showing that CRS exacerbates stroke severity. CRS-exposed mice developed larger infarcts and greater neurological deficits after ischemia/reperfusion. Mechanistically, we identified mitochondrial dysfunction as a key driver, with stress-induced mitochondrial impairment amplifying cerebral injury post-reperfusion. TSPO emerged as a central mitochondrial regulator mediating the effects of stress on stroke pathology. Pharmacological inhibition of TSPO with PK11195 alleviated CRS-aggravated brain injury, restored ATP production, and reduced apoptosis, oxidative stress, and LDH release, underscoring TSPO as a potential therapeutic target in stress-exacerbated stroke. While numerous studies have confirmed the role of TSPO in activated microglia [55, 56], our study is the first to suggest that neuronal TSPO may act by inducing mitochondrial damage. Collectively, these findings identify TSPO as a potential therapeutic target for mitigating stress-exacerbated stroke and suggest a novel strategy to improve the clinical management of ischemic stroke in high-stress populations.

#### Mitochondrial dysfunction as a central link between stress and stroke

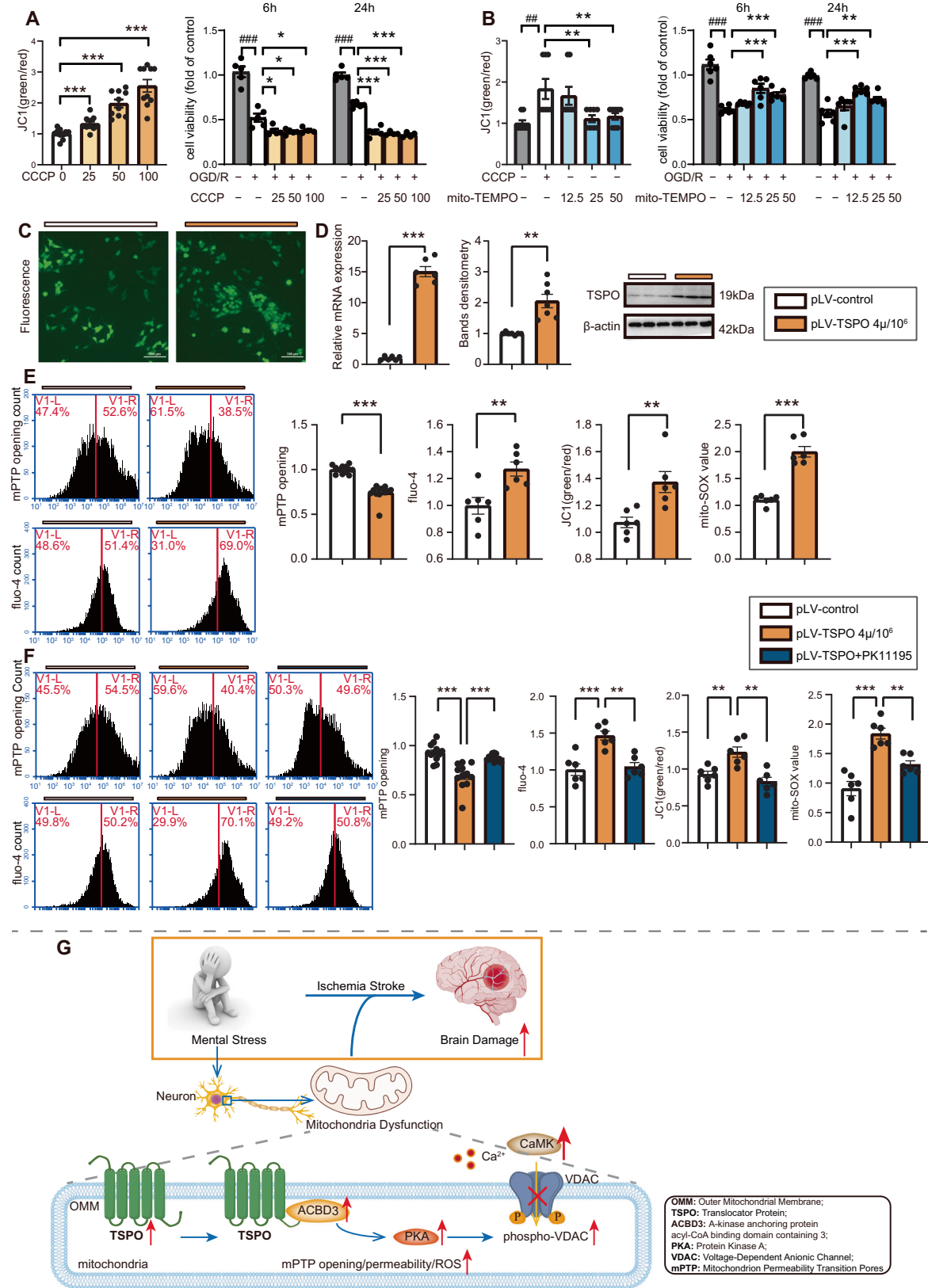
Mitochondria play a central role in both stress adaptation and ischemic injury. Psychological stress increases metabolic demands and mitochondrial workload, while chronic stress depletes ATP reserves and disrupts mitochondrial homeostasis, leading to long-term cellular dysfunction [57, 58]. Prior studies have shown that restraint stress reduces expression of mitochondrial energy-related proteins in the prefrontal cortex [59]. In line with these reports, we found that CRS markedly impaired mitochondrial function, as evidenced by reduced activity of complexes I–IV, ATPase, CS, overall ATP production, and mitochondrial biogenesis, underscoring mitochondrial dysfunction as a major consequence of chronic stress.

Mitochondria are key mediators of ischemia-reperfusion injury [48, 60]. Neurons, the most sensitive brain cells to hypoxia, depend heavily on mitochondrial ATP to sustain repair in the ischemic penumbra; however, pre-existing mitochondrial dysfunction can hinder energy restoration and lead to irreversible neuronal loss [57, 58]. In this study, we used a mitochondrial dysfunction inducer (CCCP) and a protector (Mito-TEMPO) and found that they aggravated or alleviated OGD/R-induced neuronal damage, respectively, consistent with previous studies [61–63]. These findings reinforce that mitochondrial functionality is a key determinant of ischemia-reperfusion injury and provide a basis for further exploration of the underlying regulatory factors and molecular pathways.

These findings emphasize the importance of mitochondrial function in determining stroke severity and highlight mitochondria as a potential therapeutic target in stress-exacerbated cerebrovascular injury. Although the role of mitochondria in the ischemic penumbra is well recognized, several critical questions remain. In particular, the molecular mediators and signaling pathways involved, as well as strategies to optimize mitochondrial recovery and develop mitochondria-targeted therapies, are not yet fully understood.

#### Aggravated stroke injury by TSPO as a mitochondrial mediator of stress

To identify mitochondrial regulators of stress-exacerbated ischemic injury, we used bioinformatics tools to analyze genes associated with both mental stress and ischemic stroke. After cross-referencing these genes with the mitochondrial genes cataloged in the MitoCarta3.0 database for mice, three genes were identified, including Translocator protein (TSPO), B cell leukemia/lymphoma 2 (BCL2), and DNA polymerase delta interacting protein 2 (POLDIP2). BCL2 is well-known for its role in



regulating apoptosis, and its overexpression can protect cells from death under various stress conditions, including stroke [59, 64]. POLDIP2 is involved in DNA replication and repair, which are critical processes for maintaining cellular integrity [65]. These two

molecules are more predominantly associated with cellular damage. TSPO was reported to be related to both stress-related disorders and ischemia-reperfusion induced neuronal damage [61, 66], so TSPO is considered as a potential mitochondrial

**Fig. 6 Mitochondrial Dysfunction in SH-SY5Y Cells by TSPO Overexpression Vector (pLV-TSPO) and PK11195 and Schematic Diagram.** **A** CCCP induced mitochondrial membrane potential (MMP) disruption at doses of 25, 50, and 100  $\mu$ M, and CCCP worsened OGD/R damage at 6 and 24 h after reoxygenation at doses of 25, 50, and 100  $\mu$ M. **B** mito-TEMPO alleviated CCCP increased MMP at doses of 25 and 50  $\mu$ M, with the 25  $\mu$ M dose yielding the highest viability, and mito-TEMPO decreased OGD/R induced neuron damage at 6 and 24 h after reoxygenation at doses of 25 and 50  $\mu$ M, with the 25  $\mu$ M dose yielding the highest viability. **C** TSPO overexpression vector (pLV-TSPO) was constructed and transfected effectively into SH-SY5Y cell lines. **D** TSPO overexpression vector increased the mRNA ( $p < 0.001$ ) and protein expression ( $p < 0.01$ ) in SH-SY5Y cells. **E** TSPO decreased mPTP opening ( $p < 0.001$ ), and increased intracellular  $\text{Ca}^{2+}$  by Fluo-4 staining ( $p < 0.01$ ), the ratio of green and red fluorescence in JC1 staining ( $p < 0.01$ ) and mitochondrial ROS by mito-SOX staining ( $p < 0.001$ ). **F** PK11195 increased mPTP opening ( $p < 0.001$ ), and decreased the intracellular  $\text{Ca}^{2+}$  ( $p < 0.01$ ), the ratio of green and red fluorescence in JC1 staining ( $p < 0.01$ ), and mito-ROS ( $p < 0.01$ ). Data are presented as mean  $\pm$  SEM. **G** This schematic diagram illustrates the molecular cascade triggered by mental stress that exacerbates ischemic stroke injury. Under mental stress conditions, expression of translocator protein (TSPO) is upregulated in the mitochondrial membrane. Increased TSPO interacts with ACBD3, activating the protein kinase A (PKA) signaling pathway, which subsequently phosphorylates the voltage-dependent anion channel (VDAC). This phosphorylation event disrupts mitochondrial function, leading to neuronal calcium/calmodulin-dependent protein kinase (CaMK) activation, increased intracellular calcium, oxidative stress, and neuronal injury. Collectively, this TSPO/ACBD3/PKA/VDAC1 phosphorylation/CaMK signaling pathway contributes significantly to mitochondrial dysfunction and is a critical mechanism by which mental stress aggravates ischemic brain damage.

mediator between psychological stress and ischemic stroke outcomes.

PET imaging of TSPO has been proposed as a tool for measuring psychiatric disorders, and TSPO imaging results have been associated with major depressive disorder (MDD) [62]. Beyond its role in imaging, TSPO has been reported to regulate mitochondria function in glioblastoma [63] and hepatocellular carcinoma [67]. Notably, TSPO levels in the plasma of acute ischemic stroke patients correlate with stroke severity and functional outcomes, indicating its potential as a prognostic marker [68]. Given the extensive evidence implicating TSPO in both mental stress and ischemic stroke, together with our bioinformatics screening results, we hypothesized that TSPO may be a critical mediator of stress-exacerbated brain injury. Our findings confirmed this, as the TSPO inhibitor PK11195 significantly reduced acute stroke injury, neurological deficits, ischemia-induced LDH release, ROS generation, Fas expression, and apoptotic cell death.

TSPO has been widely used as a diagnostic marker of inflammatory diseases in activated microglia [55, 56], with increased TSPO in microglia contributing to transient MCAO damage [19]. In this study, we are the first to suggest that neuronal TSPO may exert its effects by inducing mitochondrial damage. TSPO overexpression exacerbated neuronal mitochondrial dysfunction, as indicated by elevated mitochondrial membrane potential (MMP), increased intracellular calcium, enhanced mitochondrial ROS production, and reduced mitochondrial permeability transition pore (mPTP) opening—findings consistent with reports that TSPO aggravates OGD/R-induced neuronal injury in SH-SY5Y cells [61]. Our results not only highlight the therapeutic potential of TSPO inhibitors in stress-related cerebrovascular disease but also emphasize the importance of preserving mitochondrial function to mitigate the detrimental effects of stress on stroke outcomes.

#### ACBD3/PKA-VDAC pathway as downstream of TSPO in stroke

To investigate the mechanism underlying TSPO-mediated exacerbation of stroke injury, we examined its interactions with mitochondrial regulatory pathways. TSPO has been reported to interact with A-kinase anchoring protein acyl-CoA-binding domain-containing 3 (ACBD3) [26]. ACBD3 is a multifunctional protein involved in cellular signaling and membrane organization, with roles in lipid metabolism, transport, and maintenance of Golgi integrity [76]. It has also been implicated in regulating protein kinase A (PKA) activation, and the VDAC-PKA interaction is essential for preserving mitochondrial function and bioenergetic homeostasis [69].

Protein kinase A (PKA) was reported to mediate phosphorylation of the voltage-dependent anion channel (VDAC) in SH-SY5Y cell lines [26]. Phosphorylation of VDAC disrupts mitochondrial permeability and calcium homeostasis, contributing to oxidative

stress and neuronal injury [70, 71]. Previous studies have demonstrated that the VDAC1 phosphorylation alters its channel function, elevating cytosolic  $\text{Ca}^{2+}$ , activating NOX5 and disturbing redox balance through CaMKII signaling in hypothalamic glial cells [72]. The involvement of calcium ions in neuronal injury following stroke has been well studied. Accumulated calcium levels can induce mitochondrial death and affect neurological outcomes in ischemic stroke [73], and induce mitochondrial dysfunction in neurons, particularly in the context of ischemic stroke [74]. The release of extracellular mitochondrial particles from astrocytes is mediated by a calcium-dependent mechanism involving CD38 and cyclic ADP-ribose signaling, affecting neurological outcomes [44]. Additionally, downregulation of TSPO has been reported to reduce VDAC phosphorylation and oligomerization, thus improving mitochondrial function in HEK293 cells [75].

Consistent with these findings, our study demonstrated that CRS enhanced the interaction between TSPO and ACBD3, leading to increased PKA activation, elevated phosphorylation of VDAC, and subsequent activation of calmodulin-dependent kinase (CaMK), collectively exacerbating ischemic injury. Importantly, treatment with the TSPO antagonist PK11195 mitigated these effects, further confirming that TSPO promoted mitochondrial dysfunction through the ACBD3/PKA-VDAC pathway in stress-aggravated stroke pathology. In summary, our study identifies pre-stroke TSPO upregulation as a novel and critical mediator linking chronic psychological stress to exacerbated ischemic brain injury, highlighting TSPO not only as a promising imaging biomarker for stroke prognosis but also as a potential therapeutic target for precision management of CRS-related ischemic stroke.

#### CONCLUSION

Given the increasing recognition of psychological stress as an independent stroke risk factor, our findings carry meaningful translational implications. This study provides compelling evidence that chronic stress exacerbates ischemic stroke through mitochondrial dysfunction, with TSPO acting as a central mediator via the ACBD3/PKA-VDAC signaling pathway (Fig. 6G). Pharmacological inhibition of TSPO effectively attenuated CRS-induced mitochondrial impairment and reduced stroke severity, supporting its potential as a therapeutic target for stress-exacerbated cerebrovascular injury. Future research should aim to validate TSPO-targeted therapies and evaluate their clinical potential, particularly in young and middle-aged individuals, who may be disproportionately affected by the cerebrovascular consequences of chronic psychological stress.

#### Limitations

The main limitations of this study are: (i) the use of only male rodents, which may not capture sex-specific responses; future

studies will include females to assess potential dimorphisms, and (ii) the absence of neuron-specific TSPO knockout models, which limits mechanistic insight into cell-autonomous effects; developing such models will be an important next step.

### Translational values and future directions

Our findings demonstrate the translational potential of TSPO as a therapeutic target to mitigate stress-aggravated ischemic injury. By identifying TSPO-mediated mitochondrial dysfunction as a mechanistic link between chronic stress and worsened stroke outcomes, this work opens avenues for both prognostic and therapeutic applications. Clinically, TSPO could serve as an imaging biomarker to predict stroke prognosis and as a drug target for patients experiencing high stress or comorbid psychological conditions.

Future directions include: (i) investigating whether chronic stress also impairs long-term cognitive and functional recovery after stroke, as clinical studies have shown correlations between higher perceived stress, elevated cortisol, and poorer post-stroke performance; (ii) evaluating the translational potential of TSPO inhibitors such as PK11195 for reducing brain injury, with attention to efficacy and safety in clinical settings; and (iii) integrating TSPO-PET imaging with outcome prediction to enable personalized treatment strategies.

Taken together, our study identifies pre-stroke TSPO upregulation as a critical mediator linking chronic psychological stress to exacerbated ischemic brain injury, underscoring TSPO not only as a promising imaging biomarker for stroke prognosis but also as a potential therapeutic target for precision management of CRS-related ischemic stroke.

### DATA AVAILABILITY

All raw data used in this manuscript are available on reasonable request.

### REFERENCES

- Li XY, Kong XM, Yang CH, Cheng ZF, Lv JJ, Guo H, et al. Global, regional, and national burden of ischemic stroke, 1990–2021: an analysis of data from the global burden of disease study 2021. *EClinicalMedicine*. 2024;75:102758.
- Zhou H, Wang J, Zhu Z, Hu L, An E, Lu J, et al. A new perspective on stroke research: unraveling the role of brain oxygen dynamics in stroke pathophysiology. *Aging Dis*. 2024;16:2343–2353.
- Mi R, Cheng H, Chen R, Bai B, Li A, Gao F, et al. Effects and mechanisms of long-acting glucagon-like peptide-1 receptor agonist semaglutide on microglia phenotypic transformation and neuroinflammation after cerebral ischemia/reperfusion in rats. *Brain circulation*. 2024;10:354–65.
- Qiao Y, Fayyaz Al, Ding Y, Ji X, Zhao W. Recent advances in the prevention of secondary ischemic stroke: A narrative review. *Brain circulation*. 2024;10:283–95.
- Jackson AC, Rogerson MC, Murphy BM. An integrated perspective for understanding the psychosocial impact of acute cardiovascular events: a scoping review. *Heart Mind*. 2023;7:137–47.
- Ashraf F, Mustafa MS, Shafique MA, Haseeb A, Mussarat A, Noorani A, et al. Association between depression and stroke risk in adults: a systematic review and meta-analysis. *Front Neurol*. 2024;15:1331300.
- Li L, Scott CA, Rothwell PM. Association of younger vs older ages with changes in incidence of stroke and other vascular events, 2002–2018. *JAMA*. 2022;328:563–74.
- Fayyaz Al, Ding Y. Mental stress, meditation, and yoga in cardiovascular and cerebrovascular diseases. *Brain circulation*. 2023;9:1–2.
- Li F, Geng X, Ding Y. Unraveling the complex web: heart disease and stroke. *Heart Mind*. 2023;7:117–9.
- Russell G, Lightman S. The human stress response. *Nature Rev Endocrinol*. 2019;15:525–34.
- Johnson J. Effect of emotions on learning, memory, and disorders associated with the changes in expression levels: A narrative review. *Brain circulation*. 2024;10:134–44.
- Luo J, Feng L, Wang L, Fang Z, Lang J, Lang B. Restoring brain health: electro-acupuncture at GB20 and LR3 for migraine mitigation through mitochondrial restoration. *Brain circulation*. 2024;10:154–61.
- Cheng F, Yan B, Liao P, Gao H, Yin Z, Li D, et al. Ischemic stroke and the biological hallmarks of aging. *Aging Dis*. 2024;16:2908–36.
- Pola I, Ashton NJ, Antônio De Bastiani M, Brum WS, Rahmouni N, Tan K, et al. Exploring inflammation-related protein expression and its relationship with TSPO PET in Alzheimer's disease. *Alzheimer's Dement*. 2025;21:e70171.
- Martinez-Perez DA, McGlothan JL, Rodichkin AN, Abilmouna K, Bursac Z, Lopera F, et al. Amyloid- $\beta$  plaque-associated microglia drive TSPO upregulation in Alzheimer's disease. *Acta Neuropathol*. 2025;150:6.
- Selvaraj V, Stocco DM. The changing landscape in translocator protein (TSPO) function. *Trends Endocrinol Metab*. 2015;26:341–8.
- Rupprecht R, Pradhan AK, Kufner M, Brunner LM, Nothdurfter C, Wein S, et al. Neurosteroids and translocator protein 18 kDa (TSPO) in depression: implications for synaptic plasticity, cognition, and treatment options. *Eur Arch Psychiatry Clin Neurosci*. 2023;273:1477–87.
- Shi Y, Cui M, Ochs K, Brendel M, Strübing FL, Briel N, et al. Long-term diazepam treatment enhances microglial spine engulfment and impairs cognitive performance via the mitochondrial 18 kDa translocator protein (TSPO). *Nat Neurosci*. 2022;25:317–29.
- Mahemut Y, Kadeer K, Su R, Abula A, Aili Y, Maimaiti A, et al. TSPO exacerbates acute cerebral ischemia/reperfusion injury by inducing autophagy dysfunction. *Exp Neurol*. 2023;369:114542.
- Eggerstorfer B, Kim J-H, Cumming P, Lanzenberger R, Gryglewski G. Meta-analysis of molecular imaging of translocator protein in major depression. *Front Mol Neurosci*. 2022;15:981442.
- Liu Y, Chang Y, Xie X, Wang X, Ma H, Liu M, et al. PET imaging unveils neuroinflammatory mechanisms in psychiatric disorders: from microglial activation to therapeutic innovation. *Mol Neurobiol*. 2025;62:15318–35.
- Frison M, Faccenda D, Abeti R, Rigon M, Stroobé D, England-Rendon BS, et al. The translocator protein (TSPO) is prodromal to mitophagy loss in neurotoxicity. *Mol Psychiatry*. 2021;26:2721–39.
- Luo R, Wang L, Ye F, Wang Y, Fang W, Zhang M, et al. [(18)F]FEDAC translocator protein positron emission tomography-computed tomography for early detection of mitochondrial dysfunction secondary to myocardial ischemia. *Ann Nucl Med*. 2021;35:927–36.
- Turkheimer FE, Rizzo G, Bloomfield PS, Howes O, Zanotti-Fregonara P, Bertoldo A, et al. The methodology of TSPO imaging with positron emission tomography. *Biochem Soc Trans*. 2015;43:586–92.
- Desai R, East DA, Hardy L, Faccenda D, Rigon M, Crosby J, et al. Mitochondria form contact sites with the nucleus to couple prosurvival retrograde response. *Sci Adv*. 2020;6:eabc9955.
- Gatliff J, East DA, Singh A, Alvarez MS, Frison M, Matic I, et al. A role for TSPO in mitochondrial Ca<sup>2+</sup> homeostasis and redox stress signaling. *Cell Death Dis*. 2017;8:e2896.
- Su L, Zhang J, Gomez H, Kellum JA, Peng Z. Mitochondria ROS and mitophagy in acute kidney injury. *Autophagy*. 2023;19:401–14.
- Zhu Y, Haddad Y, Yun HJ, Geng X, Ding Y. Induced inflammatory and oxidative markers in cerebral microvasculature by mentally depressive stress. *Mediators Inflamm*. 2023;2023:4206316.
- Zhu Y, Klomparens EA, Guo S, Geng X. Neuroinflammation caused by mental stress: the effect of chronic restraint stress and acute repeated social defeat stress in mice. *Neurol Res*. 2019;41:762–9.
- Qiu Z, Li M, He J, Liu X, Zhang G, Lai S, et al. Translocator protein mediates the anxiolytic and antidepressant effects of midazolam. *Pharmacol Biochem Behav*. 2015;139:77–83.
- Xu Y, Zhang J, Yu L, Zhang W, Zhang Y, Shi Y, et al. Engeletin alleviates depression-like phenotype by increasing synaptic plasticity via the BDNF-TrkB-MTORC1 signalling pathway. *J Cell Mol Med*. 2023;27:3928–38.
- Chen C, Chencheng Z, Cuiying L, Xiaokun G. Plasmacytoid dendritic cells protect against middle cerebral artery occlusion induced brain injury by priming regulatory T cells. *Front Cell Neurosci*. 2020;14:1–13.
- Liu C, Yang J, Zhang C, Geng X, Zhao H. Remote ischemic conditioning reduced cerebral ischemic injury by modulating inflammatory responses and ERK activity in type 2 diabetic mice. *Neurochem Int*. 2020;135:104690.
- Geng X, Shen J, Li F, Yip J, Guan L, Rajah G, et al. Phosphoenolpyruvate carboxykinase (PCK) in the brain gluconeogenic pathway contributes to oxidative and lactic injury after stroke. *Mol Neurobiol*. 2021;58:2309–21.
- Guo S, Li F, Wills M, Yip J, Wehbe A, Peng C, et al. Chlorpromazine and promethazine (C+P) reduce brain injury after ischemic stroke through the PKC- $\delta$ /NOX/MnSOD pathway. *Mediators Inflamm*. 2022;2022:1–15.
- Guo S, Cosky E, Li F, Guan L, Ji Y, Wei W, et al. An inhibitory and beneficial effect of chlorpromazine and promethazine (C + P) on hyperglycolysis through HIF-1 $\alpha$  regulation in ischemic stroke. *Brain Res*. 2021;15:147463.
- Jiang Q, Ding Y, Li F, Fayyaz Al, Duan H, Geng X. Modulation of NLRP3 inflammasome-related-inflammation via RIPK1/RIPK3-DRP1 or HIF-1 $\alpha$  signaling by phenothiazine in hypothermic and normothermic neuroprotection after acute ischemic stroke. *Redox Biol*. 2024;73:103169.

38. Guan L, Geng X, Stone C, Cosky EEP, Ji Y, Du H, et al. PM2.5 exposure induces systemic inflammation and oxidative stress in an intracranial atherosclerosis rat model. *Environ Toxicol*. 2019;34:530–8.

39. Wang Q, Kohls W, Wills M, Li F, Pang Q, Geng X, et al. A novel stroke rehabilitation strategy and underlying stress granule regulations through inhibition of NLRP3 inflammasome activation. *CNS Neurosci Ther*. 2023;30:e14405.

40. Jiang Q, Ding Y, Li F, Rosenfeld S, Pang Q, Geng X. Inhibition of class IIa HDACs reduces neuroinflammation via NEU1-LAMP1 regulation and promotes M2 macrophage polarization in ischemic stroke. *Brain Res*. 2025;1864:149806.

41. Jiang Q, Geng X, Warren J, Eugene Paul Cosky E, Kaura S, Stone C, et al. Hypoxia inducible factor-1 $\alpha$  (HIF-1 $\alpha$ ) mediates NLRP3 inflammasome-dependent pyroptotic and apoptotic cell death following ischemic stroke. *Neuroscience*. 2020;448:126–39.

42. Yang J, Wang W, Xia H, Yu Z, Li HM, Ren J, et al. Lymphotoxin- $\alpha$  promotes tumor angiogenesis in HNSCC by modulating glycolysis in a PFKFB3-dependent manner. *Int J Cancer*. 2019;145:1358–70.

43. Lu T, Zhang J, Cai J, Xiao J, Sui X, Yuan X, et al. Extracellular vesicles derived from mesenchymal stromal cells as nanotherapeutics for liver ischaemia-reperfusion injury by transferring mitochondria to modulate the formation of neutrophil extracellular traps. *Biomaterials*. 2022;284:121486.

44. Hayakawa K, Esposito E, Wang X, Terasaki Y, Liu Y, Xing C, et al. Transfer of mitochondria from astrocytes to neurons after stroke. *Nature*. 2016;535:551–5.

45. Zhang Y, Zhang M, Zhu W, Yu J, Wang Q, Zhang J, et al. Succinate accumulation induces mitochondrial reactive oxygen species generation and promotes status epilepticus in the kainic acid rat model. *Redox Biol*. 2020;28:101365.

46. Wei W, Wu D, Duan Y, Elkin KB, Chandra A, Guan L, et al. Neuroprotection by mesenchymal stem cell (MSC) administration is enhanced by local cooling infusion (LCI) in ischemia. *Brain Res*. 2019;1724:146406.

47. Sun J, Zhang Y, Kong Y, Ye T, Yu Q, Kumaran Satyanarayanan S, et al. Microbiota-derived metabolite Indoles induced aryl hydrocarbon receptor activation and inhibited neuroinflammation in APP/PS1 mice. *Brain Behav Immun*. 2022;106:76–88.

48. An H, Zhou B, Ji X. Mitochondrial quality control in acute ischemic stroke. *J Cereb Blood Flow Metab*. 2021;41:3157–70.

49. Popov L-D. Mitochondrial biogenesis: an update. *J Cell Mol Med*. 2020;24:4892–9.

50. Fan H, Ding R, Liu W, Zhang X, Li R, Wei B, et al. Heat shock protein 22 modulates NRF1/TFAM-dependent mitochondrial biogenesis and DRP1-sparked mitochondrial apoptosis through AMPK-PGC1 $\alpha$  signaling pathway to alleviate the early brain injury of subarachnoid hemorrhage in rats. *Redox Biol*. 2021;40:101856.

51. Staduljé A, Alcaide-Corral CJ, Walton T, Lucatelli C, Tavares AAS. Analysis of PK11195 concentrations in rodent whole blood and tissue samples by rapid and reproducible chromatographic method to support target-occupancy PET studies. *Journal Chromatogr B*. 2019;1118:1119:33–39.

52. Becker G, Debatisse J, Rivière M, Crola Da Silva C, Beaudoin-Gobert M, Eker O, et al. Spatio-temporal characterization of brain inflammation in a non-human primate stroke model mimicking endovascular thrombectomy. *Neurotherapeutics*. 2023;20:789–802.

53. Su Z, Roncaroli F, Durrenberger PF, Cope DJ, Karabatsou K, Hinz R, et al. The 18-kDa mitochondrial translocator protein in human gliomas: an 11C-(R)PK11195 PET imaging and neuropathology study. *J Nucl Med*. 2015;56:512–7.

54. Koncha RR, Ramachandran G, Sepuri NBV, Ramaiah KVA. CCCP-induced mitochondrial dysfunction – characterization and analysis of integrated stress response to cellular signaling and homeostasis. *FEBS J*. 2021;288:5737–54.

55. Rossano SM, Johnson AS, Smith A, Ziaggi G, Roetman A, Guzman D, et al. Microglia measured by TSPO PET are associated with Alzheimer's disease pathology and mediate key steps in a disease progression model. *Alzheimer's Dement*. 2024;20:2397–407.

56. Nutma E, Gebro E, Marzin MC, van der Valk P, Matthews PM, Owen DR, et al. Activated microglia do not increase 18 kDa translocator protein (TSPO) expression in the multiple sclerosis brain. *Glia*. 2021;69:2447–58.

57. Kalogeris T, Bao Y, Korthuis RJ. Mitochondrial reactive oxygen species: a double edged sword in ischemia/reperfusion vs preconditioning. *Redox Biol*. 2014;2:702–14.

58. Bugger H, Pfeil K. Mitochondrial ROS in myocardial ischemia reperfusion and remodeling *Biochimica et biophysica acta. Molecular basis Dis*. 2020;1866:165768.

59. Zhao L, Liu P, Mao M, Zhang S, Bigenwald C, Dutertre C-A, et al. BCL2 Inhibition reveals a dendritic cell-specific immune checkpoint that controls tumor immuno-surveillance. *Cancer Discov*. 2023;13:2448–69.

60. Cheng Z, Wang H, Geng X, Rajah GB, Elmadhoun O, Peng G, et al. Time and tissue windows in futile reperfusion after ischemic stroke. *Aging Dis*. 2024;16:2544–52.

61. Wang K, Wang G, Zhou B. TSPO knockdown attenuates OGD/R-induced neuroinflammation and neural apoptosis by decreasing NLRP3 inflammasome activity through PPARY pathway. *Brain Res Bull*. 2022;187:1–10.

62. Meyer JH, Cervenka S, Kim M-J, Kreisl WC, Henter ID, Innis RB. Neuroinflammation in psychiatric disorders: PET imaging and promising new targets. *lancet Psychiatry*. 2020;7:1064–74.

63. Fu Y, Wang D, Wang H, Cai M, Li C, Zhang X, et al. TSPO deficiency induces mitochondrial dysfunction, leading to hypoxia, angiogenesis, and a growth-promoting metabolic shift toward glycolysis in glioblastoma. *Neuro Oncol*. 2020;22:240–52.

64. Tang H, Gamdzik M, Huang L, Gao L, Lenahan C, Kang R, et al. Delayed revascularization after MCAO ameliorates ischemic stroke by inhibiting apoptosis via HGF/c-Met/STAT3/Bcl-2 pathway in rats. *Exp Neurol*. 2020;330:113359.

65. Kashi K, Stojković G, Velázquez-Ruiz C, Martínez-Jiménez MI, Doimo M, Laurent T, et al. A unique arginine cluster in PolDIP2 enhances nucleotide binding and DNA synthesis by PrimPol. *Nucleic Acids Res*. 2021;49:2179–91.

66. Gong J, Szego EM, Leonov A, Benito E, Becker S, Fischer A, et al. Translocator protein ligand protects against neurodegeneration in the MPTP mouse model of parkinsonism. *J Neurosci*. 2019;39:3752–69.

67. Zhang D, Man D, Lu J, Jiang Y, Ding B, Su R, et al. Mitochondrial TSPO Promotes Hepatocellular Carcinoma Progression through Ferroptosis Inhibition and Immune Evasion. *Adv Sci (Wein)*. 2023;10:e2206669.

68. Chen W, Yeh H, Tsao C, Lien L, Chiwaya A, Alizargar J, et al. Plasma translocator protein levels and outcomes of acute ischemic stroke: a pilot study. *Dis Markers*. 2018;2018:9831079.

69. Yue X, Qian Y, Zhu L, Gim B, Bao M, Jia J, et al. ACBD3 modulates KDEL receptor interaction with PKA for its trafficking via tubulovesicular carrier. *BMC Biol*. 2021;19:194.

70. Meng Y, Tian M, Yin S, Lai S, Zhou Y, Chen J, et al. Downregulation of TSPO expression inhibits oxidative stress and maintains mitochondrial homeostasis in cardiomyocytes subjected to anoxia/reoxygenation injury. *Biomedicine Pharmacother*. 2020;121:109588.

71. Shoshan-Barmatz V, Pittala S, Mizrahi D. VDAC1 and the TSPO: expression, interactions, and associated functions in health and disease states. *Int J Mol Sci*. 2019;20:1–17.

72. Kim S, Kim N, Park S, Jeon Y, Lee J, Yoo S-J, et al. Tanyctic TSPO inhibition induces lipophagy to regulate lipid metabolism and improve energy balance. *Autophagy*. 2020;16:1200–20.

73. Ludhiodch A, Sharma R, Muriki A, Munshi A. Role of calcium homeostasis in ischemic stroke: a review. *CNS Neurological Disord - Drug Targets*. 2022;21:52–61.

74. Lei Q, Chen X, Xiong Y, Li S, Wang J, He H, et al. Lysosomal Ca $^{2+}$  release-facilitated TFEB nuclear translocation alleviates ischemic brain injury by attenuating autophagic/lysosomal dysfunction in neurons. *Sci Rep*. 2024;14:24836.

75. X Li, X Chen, F-Y Yang, T Shu, L Jiang, B He, et al. Effect of mitochondrial translocator protein TSPO on LPS-induced cardiac dysfunction. *Journal of advanced research*, 2024;74:455–69.

## ACKNOWLEDGEMENTS

This work was partially supported by National Natural Science Foundation of China (82301570), the Beijing Tongzhou District Financial Fund (2025), Yunhe Talent Program of Beijing Tongzhou District (2025 Xiaokun Geng/Fengwu Li), and the Science and Technology Plan of Beijing Tongzhou District (KJ2023CX022).

## AUTHOR CONTRIBUTIONS

YZ performed the main experiments and wrote the manuscript. FL assisted in conducting the experiments and revised the manuscript. OE and QP revised the manuscript. YD and XG designed and supervised the project.

## COMPETING INTERESTS

The authors declare no competing interests.

## ETHICAL STATEMENT

The ethical statement is not applicable to this article.

## ADDITIONAL INFORMATION

**Correspondence** and requests for materials should be addressed to Yuchuan Ding or Xiaokun Geng.

**Reprints and permission information** is available at <http://www.nature.com/reprints>

**Publisher's note** Springer Nature remains neutral with regard to jurisdictional claims in published maps and institutional affiliations.



**Open Access** This article is licensed under a Creative Commons Attribution-NonCommercial-NoDerivatives 4.0 International License, which permits any non-commercial use, sharing, distribution and reproduction in any medium or format, as long as you give appropriate credit to the original author(s) and the source, provide a link to the Creative Commons licence, and indicate if you modified the licensed material. You do not have permission under this licence to share adapted material derived from this article or parts of it. The images or other third party material in this article are included in the article's Creative Commons licence, unless indicated otherwise in a credit line to the material. If material is not included in the article's Creative Commons licence and your intended use is not permitted by statutory regulation or exceeds the permitted use, you will need to obtain permission directly from the copyright holder. To view a copy of this licence, visit <http://creativecommons.org/licenses/by-nc-nd/4.0/>.

© The Author(s) 2025